

Parameter determination for hypoplastic model using an inverse analysis algorithm. A case study; Northsea Sand

Détermination des paramètres pour le modèle hypoplastique à l'aide d'un algorithme d'analyse inverse, Etude de cas: Sable de la Mer du Nord

Pooyan Ghasemi

MARUM, Bremen, Germany

Vahid Galavi, Mario Martinelli

Deltares, Delft, The Netherland

Michele Calvello, Sabatino Cuomo

University of Salerno, Salerno, Italy

ABSTRACT: The hypoplastic model is an advanced constitutive model which can describe the mechanical behaviour of granular materials for a wide range of stress levels and soil densities. Niemunis and Herle (1997) improved the model performance in cyclic loading by introducing the intergranular strain stiffness. A series of valuable researches have been carried out in order to explain the role of each parameter. However, the individual roles of intergranular (small strain) parameters and the methods by which they can be estimated were rarely addressed. This paper introduces a methodology using both a parametric analysis and an automatic optimization algorithm to calibrate cyclic triaxial tests and to estimate the hypoplastic parameters, including the small strain ones. The materials being used in this study are sandy soils.

RÉSUMÉ: Le modèle hypoplastique est un modèle constitutif avancé qui peut décrire le comportement mécanique des matériaux granulaires pour une large gamme de niveaux de contraintes et de densités de sol. Niemunis et Herle (1997) ont amélioré les performances du modèle en chargement cyclique en introduisant la rigidité de déformation intergranulaire. Une série de recherches précieuses ont été menées afin d'expliquer le rôle de chaque paramètre. Cependant, les rôles individuels des paramètres intergranulaires (petite contrainte) et les méthodes permettant de les estimer ont été rarement abordés. Cet article présente une méthodologie utilisant à la fois une analyse paramétrique et un algorithme d'optimisation automatique pour calibrer les tests triaxiaux cycliques et estimer les paramètres hypoplastiques, y compris les plus faibles. Les matériaux utilisés dans cette étude sont des sols sableux.

Keywords: Hypoplastic Model, Cyclic resistance curve, Calibration, Small strain stiffness, inverse analysis

1 INTRODUCTION

The hypoplastic model is an advanced constitutive model which has been used with various numerical methods and is able to simulate

different kinds of boundary value problems, such as: simulation of static liquefaction in slopes by means of material point method (Ghasemi et al 2018 and Cuomo et al 2018b) and soil structure

interaction and pile driving simulation (Phuong et al 2016).

Accordingly, the usage of this model to reproduce the soil behavior in complex geotechnical problems is increasing. However, in all of the aforementioned research, it was shown that the right performance of the models in boundary value problems is very sensitive to the values adopted for the model parameters. Therefore, more investigation on the role of each parameter as well as on the methods for their estimation is still needed.

A series of valuable researches have been carried out in order to explain the role of each model parameters (Von Wollfersdorf, 1996). However, in previous studies the individual role of intergranular parameters and of the methods to adopt for their estimations has been rarely addressed.

Calvello et al (2017) proposed a methodology involving a combination of both parametric analysis and an automatic optimization algorithm to estimate the parameters of the numerical model of a landslide. In this paper, a slightly modified version of that methodology will be used to: identify the effect of the model parameters; investigate the model capabilities, select the right observations for the model calibration; and apply an optimization algorithm to determine the values of the model parameters.

2 HYPOPLASTIC MODEL

The model has been primarily developed for non-cohesive granular materials. The stiffness, strength, and dilation are dependent on the soil state (void ratio and stress). The basic model requires eight parameters: the critical state friction angle, φ_c , a hardness parameter, h_s , a compression law parameter, n , the reference minimum void ratio at zero mean effective stress, $e_{d0} \approx e_{min}$, the reference critical void ratio at zero mean effective stress, e_{c0} , the reference maximum void ratio at zero mean effective stress, $e_{i0} \approx e_{max}$, a parameter to control the

dependency of peak friction angle on relative density, α , and a parameter to control the dependency of soil stiffness on relative density, β .

There are also 5 other material parameters to define the material behavior at small strains: m_R is the shear modulus upon 180° strain path reversal and in the initial loading; m_T controls the initial shear modulus upon 90° strain path reversal; R_{max} relates to the size of the elastic strain range; β_r and χ are used to adjust the rate of degradation of the stiffness with strain.

As an example to show the performance of the hypoplastic model in the simulation of cyclic triaxial tests, the model parameters for a test on Hochstetten sand (Niemunis and Herle 1997) are considered. The stress controlled undrained triaxial test with initial confining pressure (p') of 300 kPa and deviatoric stress (q) of 40 kPa is simulated on a sample with the initial void ratio of 0.695 is simulated. The predicted axial strains and mean effective stress over the cycles are shown in Figure.1. It can be observed that, after a certain number of cycles, i.e. 35 cycles, the sample reaches the instability point, a dramatic drop in mean effective stress happens and the soil liquefies. However, in contrast to typical results observed in many experiments (Wichtman and Triantafyllidis, 2013), the predicted effective stress does not reach zero. Furthermore, the accumulation of axial strain takes place only towards the triaxial extension side, it does not occur in compression, and the axial strains amplitude remains almost constant. In contrast, typical results of experiments show that, after the onset of liquefaction or cyclic mobility, large axial strains happen without mobilizing any relevant shear resistance and the axial strain amplitude increases with the number of cycles.

This clearly shows the limitation of the model in predicting soil response at low-stress levels. Indeed, it must be considered that close to the instability point the soil loses its fabric and subsequently its stiffness. Therefore, low values of initial stiffness are expected. Yet, the current

formulation of the model imposes an undesirable stiffness at the onset of the unloading phase, thus leading to accumulating strains over the cycles at constant amplitudes and preventing further amplitude evolution in strains.

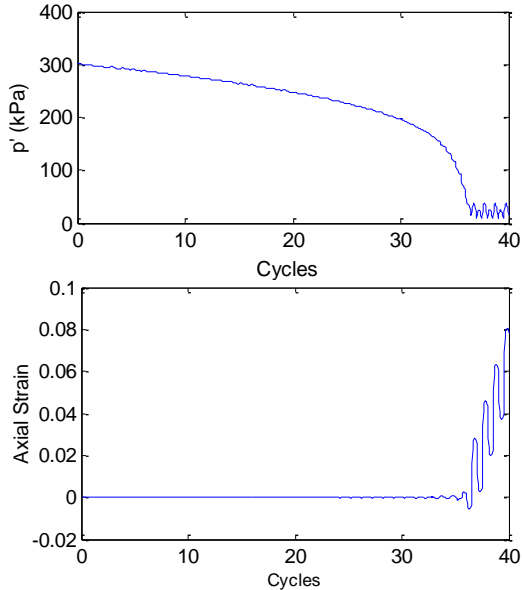


Figure 1. Hypoplastic prediction of undrained cyclic triaxial tests using the parameters of the Hochstetten sand (Niemunis and Herle, 1997)

3 MATERIAL AND METHODS

3.1 Soil properties

All of the experimental data employed in this paper are extracted from a report of Fugro (2015). In particular, this study considers the Eem/Kreftenheye sand located in the Brussels wind farm II.

The soil is characterized by a relatively high stiffness. The particle distribution curve of the material is shown in Figure.2. The soil specific density is 2.65. D_{10} and D_{60} are 0.01 mm and 0.33mm, respectively. Minimum and maximum void ratios are estimated 0.56 and 1.14, respectively.

3.2 Available data and proposed procedure

The adopted data in this study are divided into four groups. I) Laboratory index tests carried on a sample extracted from borehole BH-WSF2-5. II) Three isotropic consolidated drained tests (CID) on the samples extracted from the same borehole, with different cell pressures, i.e. 80 kPa, 160 kPa and 320 kPa, and initial void ratios equal to 0.53, 0.55 and 0.54, respectively. III) An isotropic consolidated undrained test (CIU) with local strain measurement, characterized by a confining pressure of 80 kPa and an initial void ratio of 0.57. IV) Four stress-controlled cyclic triaxial tests (CTXL), with an initial confining pressure of 80 kPa and the different values of deviatoric stresses, i.e. 28 kPa, 30 kPa, 35 kPa and 48 kPa.

The calibration procedure consists of 5 steps, in each step different types of laboratory test data are used to determine certain parameters. The overview of the process, including adopted data and calibrated parameters, is summarized in Table 1.

Based on this method, the hypoplastic model parameters are determined via a combination of three different methods of experimental results interpretation. A direct method is used to determine the parameters which can be associated with a physical feature of the soil independent from the constitutive model. Curve fitting is used for two kinds of model parameters. The first group are parameters

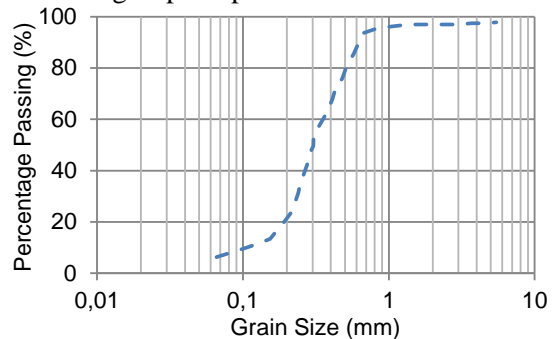


Figure 2. Particle size distribution curve for Eem/Kreftenheye sand (Fugro, 2015)

that are associated with model properties, rather than to soil physical features, and are defined only within the framework of a specific constitutive model. The second group is intrinsic soil parameters which are difficult to be determined directly from laboratory data. Both these groups of parameters are determined through inverse analysis methods and their optimal values are those that allow the best match between model response and experimental data. Finally, the surrogate curve method is used to further calibrate some of the model parameters not related to intrinsic soil characteristics. Yet, differently from the previous method, there is no unique set of parameters optimally reproducing the experimental response of the soil. The best parameter values are defined as those which fulfill the expectations of the user, not the real observed data. This concept will be further elaborated later.

According to Table 1, the direct method is used for parameters e_{i0} , e_{d0} and ϕ_c . In particular, e_{i0} and e_{d0} assigned to the model are equal to the maximum and minimum void ratios obtained from the index test. The critical friction angle is also assigned looking at the slope of the critical state line in the q-p plane of the CID tests. The rest of 5 main parameters are determined by curve fitting of $q - \varepsilon_a$ and $\varepsilon_v - \varepsilon_a$, for the

Table 1. Calibration stages along with adopted observations, variable parameter and method of parameters determination

Stage	Parameters	Used tests	Used data	Method
1	e_{i0} & e_{d0}	Index tests	γ_{\max} γ_{\min}	Direct
2	ϕ_c	CID	q-p'	Direct
3	α , β , n , h_s , e_{0c}	CID CIU	q- ε_a $\varepsilon_v - \varepsilon_a$ pwp - ε_a	Curve fitting
4	m_R , β_r , R_{\max} , χ	CIU- AD	E - ε_a	Curve fitting
5	m_R & χ	CTLX	S-N	Surrogate curve

three CID tests, as well as of $q - \varepsilon_a$ and PWP- ε_a for the CIU test. This procedure is similar to that defined by Cuomo et al. (2018a). At this stage of calibration, all of the intergranular parameters are set to zero. In the next step, the intergranular parameters m_R , β_r , R_{\max} and χ are estimated based on the curve fitting of the stiffness degradation curve $E - \varepsilon_a$.

In the next stage parameters χ and m_R are re-estimated to improve the cyclic behavior of the model. This stage adopts a surrogate curve concept. As it was explained before, the hypoplastic model is not able to predict the soil behavior at low effective stress levels. Therefore, the reproduction of real experimental curves is an impossible task. The solution is to define other surrogate goals (experimental curves) that are compatible with the model capabilities.

3.3 Curve fitting tool

The adopted SQPSO algorithm was proposed by Hosseini et al. (2014). SQPSO is a population-based evolutionary technique created by combining a Quantum Particle Swarm Optimization (QPSO) algorithm and the speciation concept. SQPSO shows a proper performance against the potential problem of being trapped in local optimum points when large search spaces are used. The performance of the algorithm to calibrate soil parameters in geotechnical problems has been evaluated by Cuomo et al. (2018a).

4 CALIBRATION AND PARAMETERS ESTIMATION

4.1.1 Static triaxial tests

Cuomo et al. (2018a) showed the performance of an inverse analysis method to determine the main parameters of the hypoplastic model using drained triaxial tests. As it was mentioned before, the values of parameters e_{i0} and e_{d0} correspond to the maximum and the minimum void ratios of the

soil obtained by index tests, 0.59 and 1.14 respectively. Parameter ϕ_c is the slope of the critical state line in the q-p plane of the CID tests, herein obtained as 35.24° . The other 5 parameters of α , β , n , h_s , and e_{oc} are determined by inverse analysis of CID and CIU tests.

In order to perform inverse analysis on three CID tests and one CIU test, the defined error function is identical to the one proposed by Cuomo et al (2018a). Two graphs of q- ε_a and ε_v - ε_a , for each CID test, as well as q- ε_a and pwp- ε_a of the CIU test are fitted against experimental results simultaneously. The error of each curve is defined based on the differences between observed and simulated values. These differences are normalized considering one percent of the maximum value of the curve. Finally, the objective function is obtained by summing all of the normalized weighted errors related to each curve. For more detailed information, the reader is referred to Cuomo et al (2018a).

The inverse analysis is performed considering the range of parameter values shown in Table 2. The table also reports the optimal values of the five considered parameters. The rest of the main parameters are assumed to be constant (as their deterministic values are already obtained). It should be underlined that all of the small strain parameters are assigned to zero at this stage.

The results of calibration of CID tests and CIU test are illustrated in Figure. 3 and Figure. 4. Adopting the estimated parameters leads to an appropriate agreement between simulation and experimental results.

The stiffness reduction curve (E- ε_a , E being q/ ε_a) obtained from CIU tests with local measurement is used to initially estimate the intergranular small strain parameters. The effect of each parameter on the stiffness reduction curve is provided in Cuomo et al. (2018b).

Table 2. Considered range for main parameters and outcome of calibration in stage 3.

Parameter	Lower bound	Upper bound	Obtained value
h_s	100×10^3	6×10^6	1.96×10^6

n	0.01	1	0.27
α	0.1	0.5	0.17
β	0.1	3.0	2.5
e_{oc}	0.59	1.14	0.78

Parameters β_r and χ influence the transition part of the curve at small to medium strains. Parameter m_R is a coefficient by which the initial small strain stiffness is calculated.

Parameter m_T is a challenging parameter to be estimated, since it has an effect only in the case of 90 degrees rotation of strain path, which does not occur in static and cyclic triaxial tests; therefore the calibration of this parameter is out of the scope of this paper and its value is assumed to be equal to half of m_R . Accordingly, with the same approach used for previous curve fitting, the E- ε_a (Figure 5) is used as the objective curve of this step to calibrate the parameters m_R , β_r , R_{max} and χ . Since this stage of calibration only affects the small strain part of the model response, the previously predicted q- ε_a and ε_v - ε_a , for the CID tests, and the q- ε_a and pwp- ε_a , for the CIU tests, still match the experimental results as before. The considered range of parameters and their optimal values are reported in Table 3.

4.2 Calibration of cyclic tests

Generally, the liquefaction resistance of the soil could be assessed by the S-N cyclic resistance curve obtained from a series of cyclic undrained triaxial tests (CTXL) with various deviatoric stress ratios. In particular, q_{cv}/σ_r depicts the normalized cyclic deviatoric stress versus the number of cycles to failure. Based on the data adopted for this case study, failure is defined when one of the following conditions is fulfilled: I) the cyclic shear strain amplitude

Table 3. Considered range for intergranular parameters and outcome of calibration in stage 4.

Parameter	Lower bound	Upper bound	Obtained value
χ	1	10	2.36
m_R	1	10	2.25
β_r	0.1	5	0.3

R_{max}	1×10^{-4}	5×10^{-4}	1×10^{-4}
-----------	--------------------	--------------------	--------------------

exceeds 3.75%; II) the excess pore water pressure exceeds 95% of the effective stress in the specimen at the start of cycling; III) the applied cyclic shear stress drops to less than 90% of the specified value.

According to section 2.2, the model is not able to reproduce the experimental results when the sample is approaching low-stress levels. Thus, the defined failure criterion of experiments in terms of axial strain and pore water pressure will not happen in the model predictions. Therefore, a new failure criterion should be defined which is compatible with the model capability. Based on this idea, the cycle in which numerical failure

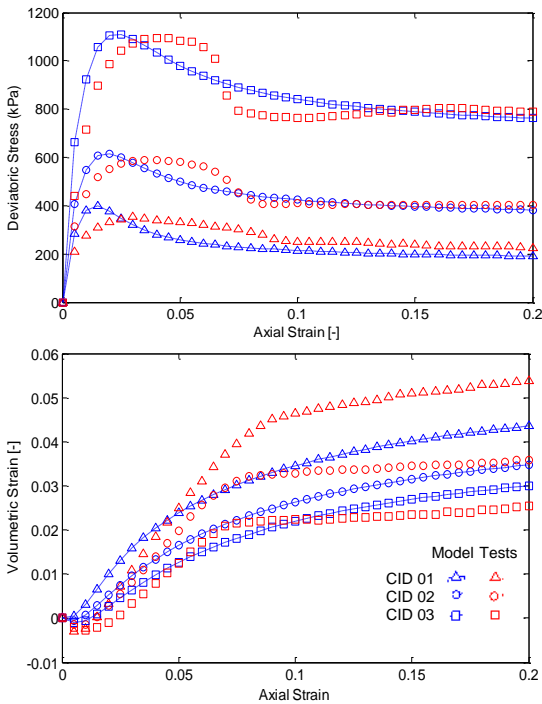


Figure 3. The outcome of 3rd step of for the three CID tests.

happens can be considered the observation to match, i.e. either the cycle at which there is a dramatic change in the trend of average axial strain or the cycle at which the pore water pressure arrives at its maximum value.

If the value of excess pore water pressure remains constant over 5 subsequent cycles, the simulation should be stopped and the failure cycle should be reported as the number of the first cycle of those 5 cycles.

Considering the aforementioned definition, the normalized cyclic deviator stress versus the cycles to the numerical failure can be plotted. This curve, which can be named artificial S-N curve, represents a surrogate curve compatible with the model capability.

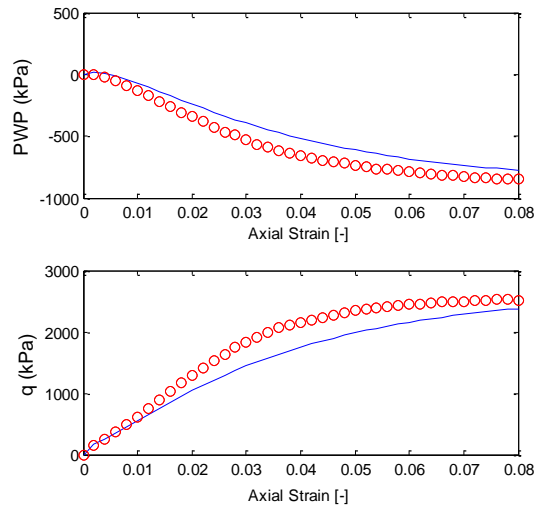


Figure 4. The outcome of 3rd step of calibration for the CIU test

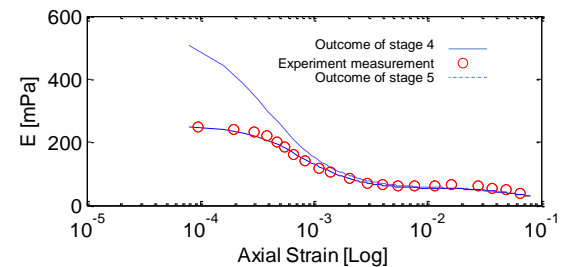


Figure 5. The outcome of 4th step of calibration in terms of one CIU test, Stiffness degradation curve

In the next step of model calibration (stage 5) the artificial S-N curve will be compared with the trend line of the S-N cyclic resistance curve derived from the experiments. As it can be seen, adopting the obtained parameters through the

calibration of static tests creates an artificial S-N curve whose slope is far steeper than the slope of the real S-N cyclic resistance curve. Therefore, some of the parameters should be modified to improve the simulation results. To this aim, a series of sensitivity analysis on the intergranular parameters have been performed. As a result, it was understood that if the parameters m_R and χ are increased, to values equals to 5.22 and 10.3 respectively, the slope of the artificial S-N curve will be similar to the S-N cyclic resistance curve of the experiments (red line in the Figure. 6).

As it was expected, adopting the new parameters value of m_R and m_T doesn't match the stiffness reduction curve of CIU tests, in a way that the predicted initial stiffness is so far higher than experiments (dash line in Figure. 5). This might be attributed to two main reasons: a shortcoming of the hypoplastic model; and a significant uncertainty in the small strain measurements of CIU experiments.

The final values of the parameters are reported in Table 4. Apart from the general output of the cyclic tests, i.e. S-N cyclic

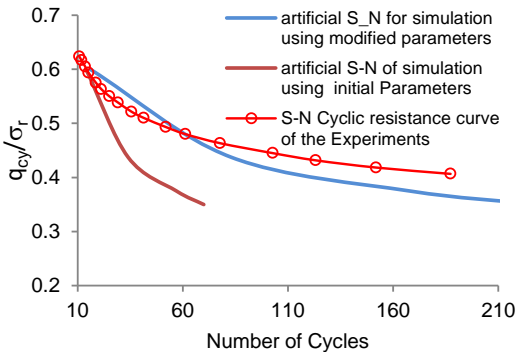


Figure 6, comparing S-N cyclic resistance curve of experiment with Artificial S-N cyclic resistance curve of simulation in terms of original and modified parameters set.

resistance curve, the outcome of calibrated model for an individual CTXL test (CTXL5 in the report of case study) is also shown in Figure. 6. In this test, the following is considered: initial void ratio of the sample equal to 0.56, $\sigma_r=80$ kPa and $q_{cv}=48$ kPa.

As it can be seen from the Figure 7, the prediction of the axial strain is significantly different from the real experimental data. In terms of predicted excess pore water pressure, as it was expected, the maximum generated pore water pressure is less than the one of recorded in the experiment. On the other hand, the pore water pressure reaches its maximum value after 12 cycles, while in the tests 18 cycles are needed.

Table 4. Final calibrated parameters of the hypoplastic model for Kreftenheye sand.

ϕ_c	e_{i0}	e_{d0}	e_{oc}	h_s
35.24	1.14	0.59	0.78	1.96×10^6
α	β	n		
0.17	2.5	0.27		
χ	m_R	m_T	R_{max}	β_r
10.3	5.22	$0.5m_R$	0.0001	0.3

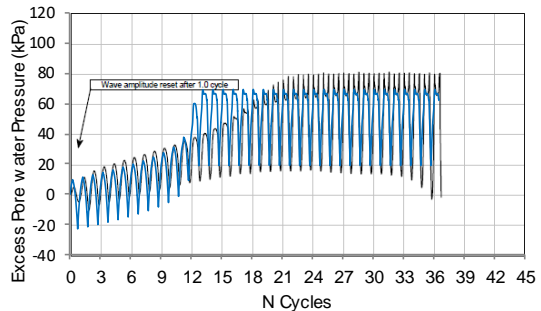
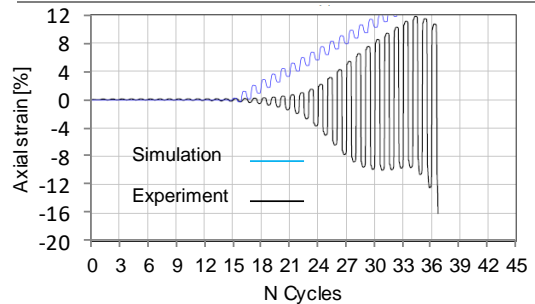


Figure 7, Simulation of CTXL5 using the calibrated parameters of the hypoplastic model

5 CONCLUSION

In this paper, a 5-step procedure has been introduced in order to determine all of the hypoplastic model parameters including the small strain ones.

Three kind of laboratory tests were adopted in the calibration procedures, which consist of drained and undrained monotonic triaxial tests as well as cyclic undrained triaxial tests performed on samples of Kreftenheye sand.

In each step of the procedure, the most relevant observations for the estimation of a certain group of parameters were used. The shortcoming of the hypoplastic model in the prediction of each adopted experimental curve was highlighted. As it was shown, the model suffers from the wrong prediction of material behavior at low stress levels, close to instability points, and for the post-failure behavior during cyclic tests.

In order to calibrate the cyclic triaxial tests, the S-N cyclic resistance curve was employed. Regarding the shortcoming of the hypoplastic model in the proper prediction of cyclic mobility and axial strain, a new failure criterion in order to identify the numerical instability was proposed, based on a new type of curve named artificial S-N curve. The slope of this curve can be compared with the one obtained by experimental data and, by matching the slopes of these two curves, the most relevant model parameters which represent liquefaction resistance of the soil can be obtained.

6 REFERENCES

- Calvello, M., Cuomo, S., & Ghasemi, P. 2017. The role of observations in the inverse analysis of landslide propagation. *Computers and Geotechnics*, 92, 11-21.
- Cuomo, S., Ghasemi, P., Calvello, M. & Hosseinezhad, V., 2018. Hypoplastic constitutive model and inverse analysis for laboratory soil tests simulation. *Proc., of 9th NUMGE Conf.*, Porto, Portugal.
- Cuomo, S., Ghasemi, P., Martinelli, M., Calvello, M., 2018, Simulation of liquefaction and retrogressive slope failure in loose cohesionless material, *ASCE Int. J. of Geomechanics* (under review).
- Fugro. (2015). *Geotechnical Report Laboratory Test Data Wind Farm Site I&II Borssele Wind Farm Zone Dutch Sector, North Sea*. Noordrop: Rijksdienst voor Ondernemend Nederland.
- Herle, I., and Gudehus, G. 1999. Determination of parameters of a hypoplastic constitutive model from properties of grain assemblies. *Mechanics of Cohesive-frictional Materials*, 4(5), 461-486.
- Hosseinezhad, V., Rafiee, M., Ahmadian, M., and Ameli, M. T., 2014, Species-based quantum particle swarm optimization for economic load dispatch. *Int. J. of Electrical Power and Energy Systems*, 63, 311-322.
- Niemunis, A., and Herle, I. ,1997, Hypoplastic model for cohesionless soils with elastic strain range. *Mechanics of Cohesive-frictional Materials*, 2(4), 279-299.
- Phuong, N. T. V., Van Tol, A. F., Elkadi, A. S. K., and Rohe, A., 2016. "Numerical investigation of pile installation effects in sand using material point method." *Computers and Geotechnics*, 73, 58-71.
- Von Wolffersdorff, P. A. (1996). A hypoplastic relation for granular materials with a predefined limit state surface. *Mechanics of Cohesive frictional Materials: An International Journal on Experiments, Modelling and Computation of Materials and Structures*, 1(3), 251-271.
- Wichtmann, T., Triantafyllidis, T., 2016. An experimental database for the development, calibration and verification of constitutive models for sand with focus to cyclic loading: part I—tests with monotonic loading and stress cycles." *Acta Geotechnica* ", 11(4), 739-761.